ICANS-VI

INTERNATIONAL COLLABORATION ON ADVANCED NEUTRON SOURCES

June 27 - July 2, 1982

MONTE CARLO STUDY OF THE ENERGY DEPOSITION OF A FLUX OF SPALLATION NEUTRONS IN VARIOUS SAMPLES

M. Pepin
Schweizerisches Institut für Nuklearforschung
CH-5234 Villigen, Switzerland

ABSTRACT

The flux of spallation neutrons produced on a sample by a 10 μA beam of 520 MeV protons incident on a 25 cm long cylindrical lead target of 7.7 cm radius was estimated with the Monte Carlo codes HET and O5R. In order to save computing time, the simulation was done in two steps, and the number of high-energy neutrons in the region of interest could be enhanced at the end of the first step. The calculated flux was compared with the values measured by S. Cierjacks, M.T. Rainbow, M.T. Swinhoe, and L. Buth at 590 MeV. The energy deposed in the sample by nuclear reactions above 15 MeV and by elastic recoils was estimated for the materials Be, C, Al, Fe, Cu, W, Pb, Bi and D_2O. For a 10 μA incoming beam, the total energy deposition varies between 1.02×10^{-4} cal/cm^{3}sec for Bi and 3.30×10^{-4} cal/cm^{3}sec for D_2O. The fraction of this energy which is deposed through elastic recoils varies from 6 % for Bi to 88 % for D_2O.

MONTE CARLO STUDY OF THE ENERGY DEPOSITION OF A FLUX OF SPALLATION NEUTRONS IN VARIOUS SAMPLES

M. Pepin
Schweizerisches Institut für Nuklearforschung
CH-5234 Villigen, Switzerland

1. INTRODUCTION

The design of high-intensity spallation neutron sources requires a better knowledge of the heating effects of the neutron flux on the components of the source than is now available. In order to learn more about these effects, an experiment to measure the heat-up of samples of the nine materials Be, C, Al, Fe, Cu, W, Pb, Bi and D_2O in the flux of the TRIUMF neutron source is being planned as a collaboration between KFA Jülich and SIN, and will be carried out at the end of this year.

In preparation for this experiment we have used the Monte Carlo codes HET [1] and O5R [2] to estimate

(i) the neutron flux expected at the sample position in conditions approximating the planned experiment, and

(ii) the expected values of heat deposition through high-energy nuclear interactions and through elastic recoils for all nine sample materials.

2. GEOMETRY OF THE SOURCE

The geometry assumed for the computation is a simplified version of the TRIUMF neutron source (see Fig. 1). In particular, the walls containing the moderator baths are omitted and only a central volume of 75 x 100 x 100 cm^3 is considered.

The production target is a lead cylinder, 25 cm in length and of 7.7 cm radius. It is surrounded by a H_2O/D_2O moderator assembly which includes an iron shielding block above the target and two vertical irradiation shafts. In the planned experiment, the samples will be placed in the rectangular shaft to the side of the target. To obtain sufficient statistics, a 5 x 5 x 2 cm^3 sample was chosen for the Monte Carlo run, although the experiment will use samples approximately one order of magnitude smaller in volume. The relative positions of target and sample are shown in Fig. 2.

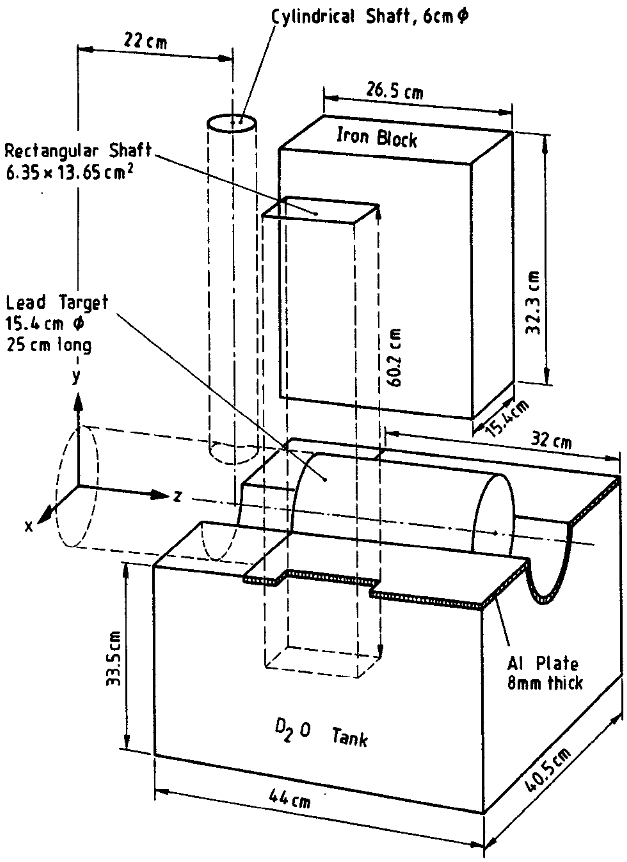

Fig. 1
Simplified geometry of the central region of the TRIUMF neutron source, as used in the Monte Carlo study.

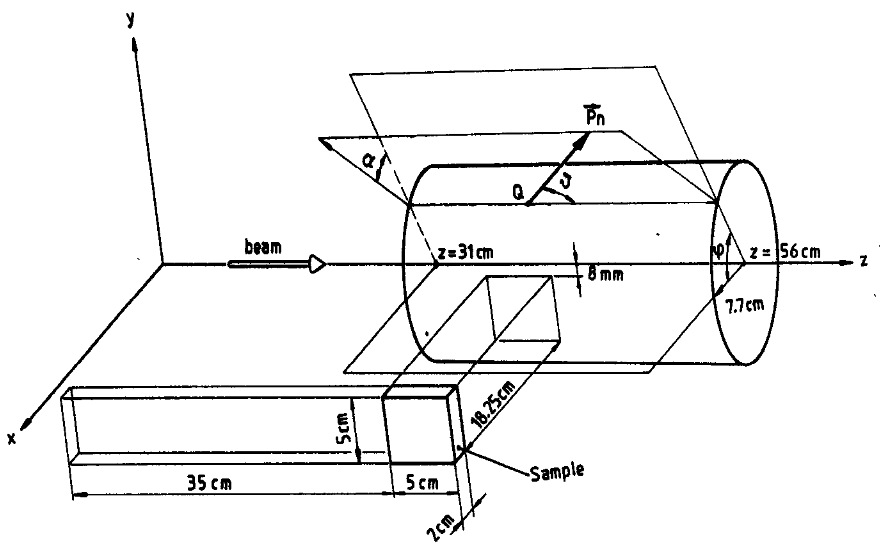

Fig. 2
Sketch showing the position of the sample with respect to the lead target, and the definition of the kinematic parameters used to describe the escaping neutrons.

3. ORGANISATION OF THE RUN

The calculation was done in five steps, as follows:

(i) HET run for the Pb target,
(ii) fit to the escape spectrum,
(iii) high-energy neutron flux ($E > 15$ MeV),
(iv) low-energy neutron contribution (10 eV $< E < 15$ MeV),
(v) energy deposition.

4. HET RUN FOR THE LEAD TARGET

The beam used in the calculation is a 15 mm radius, $300\ \pi \times 250\ \pi$ mm mrad beam of 520 MeV protons. One hundred thousand cascades were generated and followed to the point where the particles escape from the lead. The yield of high-energy escapes was 0.627 ± 0.003 neutrons and 0.006 ± 0.0002 protons per incoming proton. There were also $(9 \pm 1) \times 10^{-4}$ positive pion and $(5 \pm 1) \times 10^{-4}$ negative pion escapes per incoming proton.

The energy deposition in the target was 360 MeV per incoming proton, corresponding to 860 cal/sec for a 10 μA beam.

5. FIT TO THE ESCAPE SPECTRUM

It is clear that a straightforward one-pass Monte Carlo simulation of the whole target-moderator-sample system requires a prohibitively large number of incoming protons in order to obtain a meaningful spectrum of neutrons at the sample. We therefore fitted the spectrum of escaping neutrons and regenerated a large number of escapes in the region where the neutron has some chance to make a contribution to the flux on the sample. Propagation of neutrons escaping outside this region could be dropped.

The kinematic parameters used in this fit are defined in Fig. 2. The lead target was divided lengthwise into five sections of 5 cm each. For each section, cuts were defined in the polar angle ϑ between the neutron momentum $\vec{p}_n$ and the z-direction; the cuts were used to reject events too strongly forward or backward peaked (see Fig. 3). The retained events (about 30 % of the total number of escapes) were used to plot the following distributions:

(i) z-coordinate of the escape point Q
(ii) polar angle ϑ for the five intervals of z
(iii) kinetic energy E and angle α for 12 subregions in the z-ϑ space.

These distributions were used to generate escaping neutrons. For the azimuthal angle φ of the escape point, an isotropic distribution

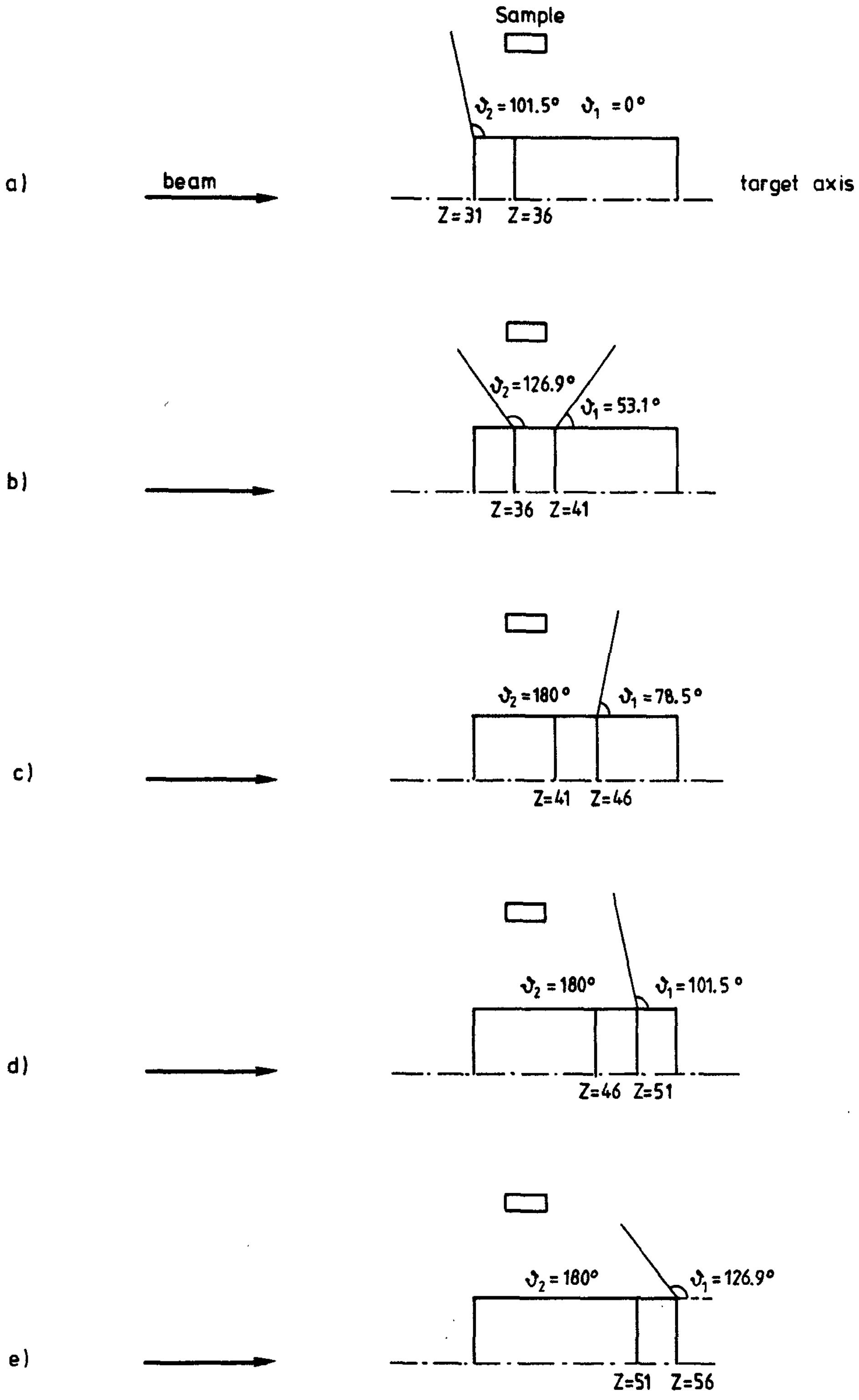

Fig. 3
Limiting values ϑ_1 and ϑ_2 of the polar angle ϑ for the five sections of the lead target. These cuts define the neutron escapes selected for fitting.

within a 36-degree sector whose bissecting line points to the sample center, was assumed.

For simplification, the propagation of protons and pions was abandoned from this point on.

6. HIGH-ENERGY NEUTRON FLUX AT SAMPLE POSITION

In order to allow the treatment of D_2O, which is present both in the moderator bath and as one of the nine samples, a Glauber type model written by F. Atchison [3] was linked into the HET code, and was used instead of the intranuclear cascade evaporation model for non-elastic collisions with deuterium.

The code was then used to simulate the propagation of 10^5 neutrons from the escape point through the moderator and onto the sample. As a check, 5×10^4 neutrons were also generated from each of the two adjacent 36-degree sectors. About 12'800 neutrons hit the sample and could be used to estimate the shape of the high-energy spectrum. Scaling back to compensate for the re-generated particles, we obtained an absolute flux of 256 ± 5 high-energy neutrons on the sample per 10^5 incoming protons (quoted error is statistical only). The contribution of the two "adjacent" sectors to this number is 7 %, so that the contribution of even more distant sectors can certainly be neglected.

As an additional check on the validity of our fits and cuts, a small number of cascades were generated and followed in one pass through the whole system. The result obtained from this run was 300 ± 55 neutron hits on the sample per 10^5 incoming protons.

7. LOW-ENERGY NEUTRON CONTRIBUTION

The first HET pass for the lead target also produced 9.37 low-energy neutrons per incoming proton, which were not transported further by HET. The propagation of this flux out of the lead and through the moderator was followed with O5R, which was also used to transport the low-energy neutrons produced in the moderator. The total flux of low-energy neutrons ($10\ eV < E < 15\ MeV$) on the sample amounts to 6121 ± 80 neutrons per 10^5 incoming protons (neutrons produced in the moderator contribute less than 1 % to this value).

The neutron spectrum obtained at sample position (low- and high-energy ranges combined) is given in Table I; the Table also shows the flux of neutrons at target surface and at approximately 90° ($-0.2 < \cos\vartheta < 0.2$).

Table I

Monte Carlo computed spectra of neutrons at sample position, and at target surface

Energy Interval (MeV)	Flux on Sample (n/p MeV cm^2)	90^0 Flux at Target Surface (n/p MeV sr)
10^{-5} - 10^{-4}	3.53	
10^{-4} - 10^{-3}	3.94×10^{-1}	
10^{-3} - 10^{-2}	4.11×10^{-2}	17.8×10^{-2}
10^{-2} - 10^{-1}	5.05×10^{-3}	41.7×10^{-2}
0.1 - 1.0	6.13×10^{-4}	41.0×10^{-2}
1.0 - 1.5	1.87×10^{-4}	21.7×10^{-2}
1.5 - 2	1.27×10^{-4}	15.1×10^{-2}
2 - 3	9.45×10^{-5}	89.9×10^{-3}
3 - 5	3.38×10^{-5}	31.7×10^{-3}
5 - 7	1.55×10^{-5}	13.1×10^{-3}
7 - 10	9.81×10^{-6}	65.1×10^{-4}
10 - 15	4.18×10^{-6}	25.5×10^{-4}
15 - 25	3.33×10^{-6}	12.87×10^{-4}
25 - 35	1.77×10^{-6}	6.80×10^{-4}
35 - 45	1.18×10^{-6}	4.65×10^{-4}
45 - 55	8.94×10^{-7}	3.55×10^{-4}
55 - 65	6.28×10^{-7}	2.65×10^{-4}
65 - 75	5.12×10^{-7}	2.03×10^{-4}
75 - 85	3.74×10^{-7}	1.55×10^{-4}
85 - 95	3.17×10^{-7}	1.23×10^{-4}
95 - 105	2.62×10^{-7}	9.55×10^{-5}
105 - 115	1.86×10^{-7}	7.36×10^{-5}
115 - 135	1.30×10^{-7}	5.73×10^{-5}
135 - 155	1.00×10^{-7}	2.75×10^{-5}
155 - 175	5.75×10^{-8}	1.59×10^{-5}
175 - 195	3.28×10^{-8}	9.15×10^{-6}
195 - 215	2.59×10^{-8}	4.58×10^{-6}
215 - 235	1.51×10^{-8}	2.38×10^{-6}
235 - 255	1.31×10^{-8}	1.59×10^{-6}
255 - 175	5.04×10^{-9}	0.32×10^{-6}
275 - 295	3.84×10^{-9}	
295 - 315	2.32×10^{-9}	
315 - 335	1.52×10^{-9}	

In Fig. 4 the flux obtained at sample (plotted with circles) is compared to the flux emitted above 15 MeV at target surface (black dots). One sees how the material between target and sample selectively depresses the less energetic part of the flux. The results are also compared to the values measured at 90^0 by S. Cierjacks,

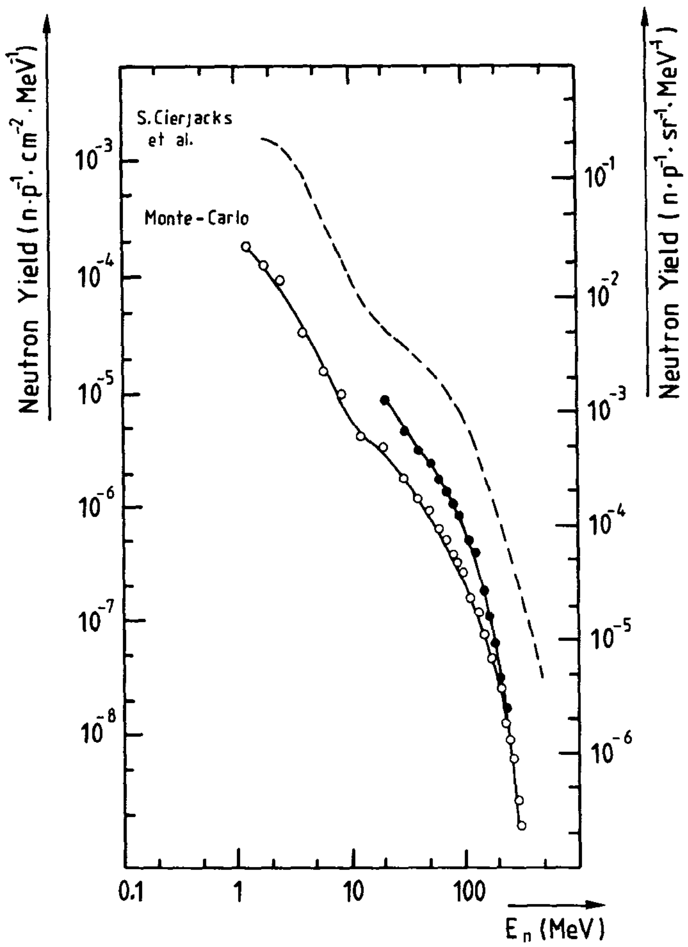

Fig. 4
Monte Carlo computed energy spectra of the neutrons emitted at 90° ($-0.2 < \cos\vartheta < 0.2$) from the target surface (black dots, right vertical scale), and of the neutrons incident on the sample (circles, left vertical scale), for an incoming proton energy of 520 MeV. For comparison, one of the spectra measured by S. Cierjacks et al. [4] is also shown (dashed line, right vertical scale; 90° neutrons, integrated over the first 35 cm of a thick lead target, incoming proton energy 590 MeV).

M.T. Rainbow, M.T. Swinhoe and L. Buth [4] for 590 MeV incoming protons and a thick lead target (dashed line). Our calculated flux at target surface is weaker than the measured one by a factor varying between about 5 (at 15 MeV) and 20 (at 300 MeV). Another short HET run indicates that the calculated yield of neutrons increases by 24 % when the incoming proton energy is taken to be 590 MeV.

8. ENERGY DEPOSITION

Two main processes were considered up to now for estimating the energy deposition in the sample:

(i) non-elastic interactions of the neutrons with the sample nuclei at higher energies, and

(ii) recoils of the sample nuclei following elastic collisions.

The energy deposition of non-elastic interactions was estimated by making, for each sample material, a HET run with incident neutrons generated according to the high-energy part ($E > 15$ MeV) of our spectrum. The history tapes were then examined with the heat depositon analysis programme ENDEN5 [5].

The number of recoils from elastic collisions was obtained from our neutron spectrum and from the compilation of neutron cross-sections by D.I. Garber and R.R. Kinsey [6]. The total energy deposition through this mechanism depends on the angular distribution of the recoils. In this estimation we assumed, as a simple model, a linear distribution of the cosine μ of the center-of-mass scattering angle,

$$P(\mu) = \frac{1}{2}\,(1 + 3.f_1.\mu)$$

with f_1 values taken from the ENDF/B data. For lack of better data, it was also assumed that the f_1 values at 20 MeV were valid at all higher energies. The results are shown in Table II.

Table II

Heat deposition from nuclear reactions above 15 MeV E_r and from elastic recoils E_{el} for a 10 µA incoming proton beam, and corresponding initial rate of sample heat-up for nine materials.

	Energy deposition (cal/10 µA · sec · cm^3)			$\frac{dT}{dt}$
	E_r	E_{el}	$E_r + E_{el}$	(^{o}C/sec)
Be	1.08×10^{-4}	1.78×10^{-4}	2.86×10^{-4}	3.5×10^{-4}
C	0.99×10^{-4}	1.03×10^{-4}	2.02×10^{-4}	7.6×10^{-4}
Al	0.99×10^{-4}	0.42×10^{-4}	1.41×10^{-4}	2.4×10^{-4}
Fe	2.32×10^{-4}	0.28×10^{-4}	2.60×10^{-4}	3.1×10^{-4}
Cu	2.27×10^{-4}	0.32×10^{-4}	2.59×10^{-4}	3.1×10^{-4}
W	2.20×10^{-4}	0.12×10^{-4}	2.32×10^{-4}	3.8×10^{-4}
Pb	1.06×10^{-4}	0.08×10^{-4}	1.14×10^{-4}	3.3×10^{-4}
Bi	0.96×10^{-4}	0.06×10^{-4}	1.02×10^{-4}	3.5×10^{-4}
D_2O	0.41×10^{-4}	2.89×10^{-4}	3.30×10^{-4}	3.0×10^{-4}

A noteworthy feature of these results is that the energy deposition through elastic recoils is the major contribution for light nuclei, and remains a sizeable effect for medium-heavy ones (e.g. 12 % for copper).

ACKNOWLEDGEMENTS

I owe a great deal to F. Atchison, who suggested the "guided" Monte Carlo method in order to make this study feasible on a VAX-11/780 computer, and who supplied the Glauber model and heat analysis programmes [3,5]. His advice and help during the run were most valuable, and he suggested many improvements to the writing of this paper.

REFERENCES

[1] HETC, ORNL 4744.
[2] O5R, ORNL Report CCC-161/NMTC and CCC-17.
[3] F. Atchison, private communication.
[4] S. Cierjacks, M.T. Rainbow, M.T. Swinhoe, and L. Buth, Primärbericht KfK 3097 B, Fig. 6.
[5] F. Atchison, ENDEN5, private communication.
[6] D.I. Garber and R.R. Kinsey, Neutron Cross Sections, BNL 325.